GSA Data Repository 2017096

METHODS

The Po River lowstand wedge and associated strata have been investigated with 1500 km of high-resolution multichannel and chirp seismic profiles. Key stratigraphic surfaces and seismic facies were correlated, loop-tied, and mapped using Petrel®. Age constraints came from calibrated ^{14}C dates, tephra identification, and dated key bio-events (see the following section) from the continuous recovery PRAD 1-2 borehole, located in the distal region of the wedge. The borehole analyses were tied to the seismic lines by using a sound propagation velocity of 1500m sec^{-1}, as suggested by sonic log analyses (Maselli et al., 2010). The progradation and the Sediment Accumulation Rate (SAR) have been calculated as horizontal migration and vertical thickness, respectively, of each clinothem at the corresponding shelf-edge divided by the correspondingly interval of time.

We conducted our shelf-edge trajectory analysis in due consideration of the fact that the rollover point (offlap break of Jervey, 1988) at the topset–foreset transition of a clinothem can occur in shelfal marine environments and thus might not necessarily represent the shoreline (i.e., the shelf-edge rollover point, at best, approximates the shoreline position: e.g. Patruno et al., 2015; Pellegrini et al., 2015 and discussion there in). When the shoreline is not at the clinothem rollover point, the maximum regression surface (MRS) would not coincide with the maximum seaward position of the shoreline (as defined by Helland Hansen and Martinsen, 1996), although, more importantly, it still does conform to the more fundamental definition of the MRS as the surface that separates progradational-aggradational stacking from retrogradation (Neal and Abreu, 2009) and as the surface that occurs at the top of the youngest marine clinoform in the depositional sequence that is lapped onto by transgressive strata (Catuneanu et al., 2009).

MULTICHANNEL SEISMIC LINES

The Po River lowstand wedge comprises distinctive clinothems (type A, B, and C). These 100's-meter-thick clinothems are systematically stacked and characterized by different bottomset deposits interpreted as mass-transport complexes (MTCs in type A clinothems) and distributary channel-lobe complexes (DLCs in Type B clinothems) as illustrated in Fig. DR1.

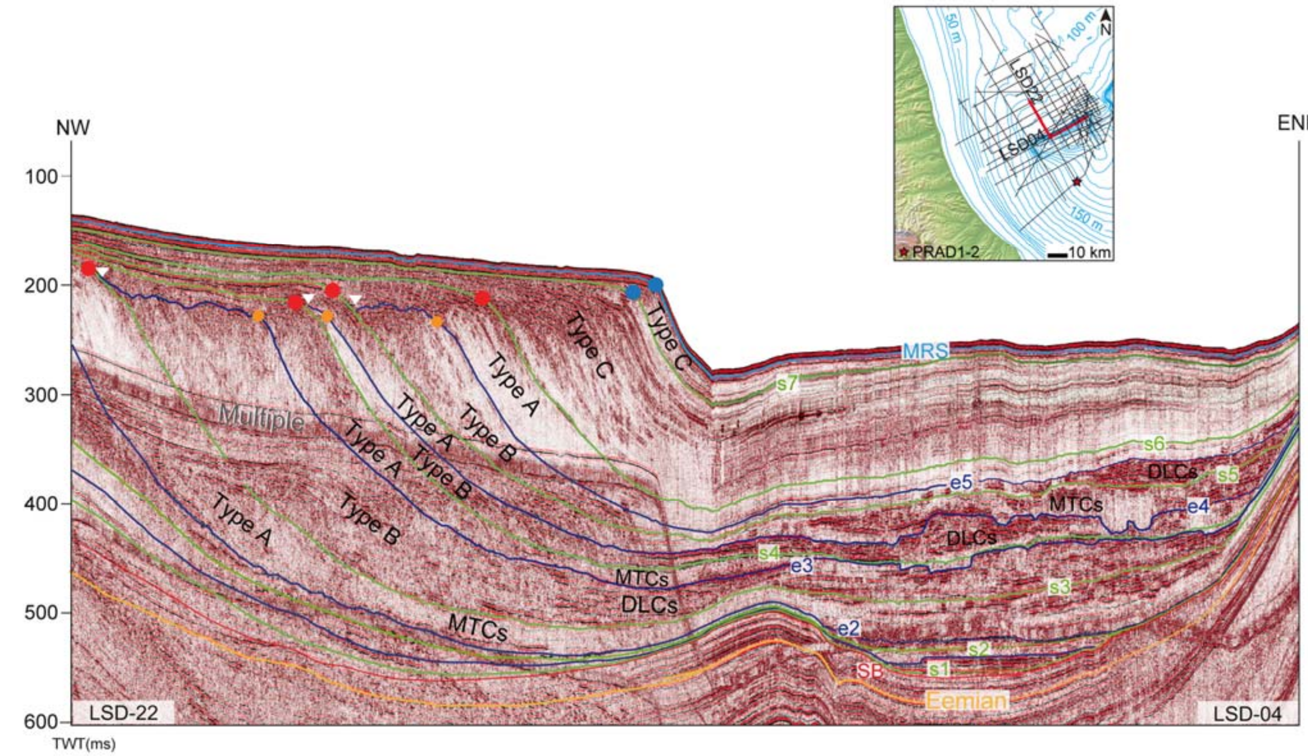

Figure DR1: Cross-section of multichannel seismic profiles showing the geometry of the distinctive type of clinothems and associated bottomset deposits. Note the alternation between mass-transport complexes (MTCs) and distributary channel-lobe complexes.

CHRONOLOGY OF THE PRAD 1-2 BOREHOLE

The chronology of the investigated interval of borehole PRAD1-2 relies on the integration of both new data and information already available in literature (Table DR2; Asioli et al., 2001; Piva et al., 2008) ^{14}C AMS dates, accompanied by tephrochronology on macro and cryptotephra (Bourne et al., 2010) as well as on bio- and event-stratigraphic control points (Piva et al., 2008; Ridente et al., 2009). The six radiocarbon dates available from literature (Table DR2) were performed on samples of monospecific benthos (either *Elphidium crispum* or *Hyalinea balthica*) at the Poznan Radiocarbon Laboratory, Poland, and the five new ones were performed on samples of monospecific benthos (either *Elphidium crispum*, *or Glandulina laevigata*) at the NOSAMS National Ocean Sciences Accelerator Mass Spectrometry Facility, Department of Geology and Geophysics, Woods Hole Oceanographic Institution, USA and at Poznan Laboratory. The specimens were picked up from the size fraction >0.250 mm.

For the present study all the ages were calibrated using the online Calib 7.1.0 Radiocarbon Calibration Program (Stuiver and Reimer, 1993) and the calibration data set Marine13.14c by Reimer et al. (2013). ΔR (reservoir) of 135.8 years with a standard deviation of 40.8 years, was constrained by two sites on the western side of the Adriatic: one from the Northern Adriatic (487 years, Rimini) and another from the Southern Adriatic (483 years, Barletta), avoiding data from Dalmatia and Croatia (Rovigne, 262 and 254 years, respectively), because these data are from a different geological context dominated by karst structures. We assume that, during the last climate cycle at least, the area where PRAD1-2 borehole was recovered was mostly influenced by the western Adriatic catchment area.

Level	Core depth (mbsf)	Lab. n.	^{14}C age (yr BP)	Species	Calibrated age (range) yr BP
PRAD1-2 S8 cm 40-42	5.976	Poz-16129	14930 ± 90	*E. crispum*	17226 - 17845
PRAD1-2 S10 cm 60-62	7.80	Poz-16130	16530 ± 100	*E. crispum*	18991 - 19569
PRAD1-2 S12 cm 0-2	8.80	OS-121214	17000 ± 50	*E. crispum*	19628 - 20065
PRAD1-2 S13 cm 0-2	9.60	OS-121280	18200± 85	*E. crispum*	21024 - 21681
PRAD1-2 S14 cm 10-12	10.50	OS-121215	19200± 40	*E. crispum*	22376 - 22680
PRAD1-2 S15 cm 20-22	11.40	OS-121496	20300±110	*E. crispum*	23471 - 24098
PRAD1-2 S15 cm 70-72	11.90	Poz-25365	21140 ± 180	*G. laevigata*	24301 - 25314
PRAD1-2 S16 cm 50-52	12.48	OS-121281	22100± 130	*E. crispum*	25602 - 26076
PRAD1-2 S16 7/8	12.78	Poz-25366	20990 ± 260	*E. crispum*	23978 - 25313
PRAD1-2 S17 cm 60-62	13.40	Poz-16131	24130 ± 150	*E. crispum*	27458 - 27959
PRAD1-2 S17 cm 60-62	13.40	Poz-16132	23390 ± 150	*H. balthica*	26741 - 27505
PRAD1-2 S19 cm 40-42	14.8	Poz-17321	28960 ± 270	*E. crispum*	31536 - 33163

Table DR2: Dates available from the literature (labeled Poz; from Piva et al., 2008) and six new dates performed for this study (labeled OS and Poz-25365); the ages are expressed as range 2σ.

Five tephra layers determined by geochemical analysis occur within the investigated interval offering an independent cross check for the radiocarbon dates, and were included in the age model as additional control points. The five tephra were analyzed by Bourne et al. (2010) and the reader is referred this paper for further details about the tephra ages obtained independently from the ^{14}C dates above described. Finally, three dated bio-events were used as additional control points (Piva et al. 2008) were used for the uppermost 2 m of the PRAD 1-2 borehole section and they include: 1) the Last Occurrence of the planktic foraminifer *Globorotalia inflata* at 6 cal. kyr BP, a key marker recognized in the whole Adriatic basin and pre-dating the attainment of the maximum flooding during the Holocene (Trincardi et al., 1996); 2) the recognition of the time-equivalent deposit of Sapropel 1 in the eastern Mediterranean, a major oceanographic event centered at 8.5 cal. kyr according to the astronomical tuning by Lourens (2004); and 3) the paleoenvironmental change related to the end of the GS-1 event well recognized in the Adriatic basin and dated at 12 cal kyr by Piva et al. (2008). In Table DR3 all the available control points are listed. The control points obtained from of the radiocarbon ages are mid points.

Sample top (m)	Age range (yr BP)	Source	Reference		Control points	SAR (cm/ka)
0	0	modern time	Piva et al. (2008)	accepted	0	10
0.6	6000	LO *G. inflata*	Piva et al. (2008)	accepted	6000	28
1.288	8500	Sapropel equivalent 1	Piva et al. (2008)	accepted	8500	15
1.8	12000	Top GS-1	Piva et al. (2008)	accepted	12000	18
2.18	14320 - 13900	Neapolitan Yellow Tuff	Bourne et al. (2010)	accepted	14110	111
5.976	17226 - 17845	^{14}C	Piva et al. (2008)	accepted	17540	108
7.8	18991 - 19569	^{14}C	Piva et al. (2008)	mean	19275	420
7.84	19480 - 19050	Greenish/Verdoline	Bourne et al. (2010)	mean		
8.8	19628 - 20065	^{14}C	this study	accepted	19498	43
9.6	21024 - 21681	^{14}C	this study	accepted	21350	76
10.50	22376 - 22680	^{14}C	this study	accepted	22528	72
11.40	23471 - 24098	^{14}C	this study	accepted	23780	160
12.48	25602 - 26076	^{14}C	this study	rejected		
12.78	23978 - 25313	^{14}C	Piva et al. (2008)	accepted	24725	25
13.32	28255 - 26302	VRa	Matthews et al. (2015)	mean	27200	27
13.4	26741 - 27505	^{14}C	Piva et al. (2008)	mean		
14.8	31536 - 33163	^{14}C	Piva et al. (2008)	accepted	32350	15
14.94	33965 - 32630	Codola (base)	Matthews et al. (2015)	accepted	33300	26
16.53	39390 - 39170	Campanian Ignimbrite	Bourne et al. (2010)	accepted	39500	

Table DR3: The age model of the study encompassing the ^{14}C dates on benthic species and tephra layers.

The radiocarbon dating at 12.48 m has been rejected as producing an inversion with the underlying age. The higher value may reflect interval-time with river input of older carbon-rich sediments. In two cases the age provided by ^{14}C has shown an age overlapping with the age of a tephra positioned very close (within 4 to 8 cm), and therefore, to avoid possible distortions due to a too short integrating time interval, depth and age of the control points were calculated by averaging the values of the levels above and below. The age of the surfaces has been calculated by linear interpolation between two successive control points, assuming constant the sediment accumulation rates between them (Table DR4). Finally, the sediment accumulation rates (SAR) have been calculated for each discrete interval.

SURFACE	Depth in PRAD1-2 (m)	AGE (cal.kyr BP)
MRS	2.5	14.4
s7	4.0	15.8
s6	6.5	18.0
e5	7.0	18.6
s5	7.5	19.0
e4	8.1	19.3
s4	8.4	19.4
e3	9.3	20.6
s3	9.5	21.1
e2	11.0	24.2
s2	12.8	24.7
e1	13.75	28.4
s1	14.0	29.4
SB	14.6	31.8
top Eemian	30.7	125.0

Table DR4: Depth of the surfaces tied to PRAD1-2 borehole and corresponding age.

SEISMIC GRID CALIBRATION THROUGH CHIRP PROFILE

The key stratigraphic surfaces are tied to the PRAD1-2 borehole with a vertical resolution of 0.3-0.5 m (Fig. DR5). Orange horizon represents the top of Eemian stage; red horizon shows the sequence boundary (SB) at the base of the Po River lowstand wedge; blue horizons are on top of type B clinothems while green horizons represent surfaces on top of type A and type C clinothems (except the younger type C clinothem that is topped by the MRS, light blue horizon). The age control of the key surfaces comes from the age model discussed above, except for the age of the top Eemian surface which comes from Maselli et al. (2010).

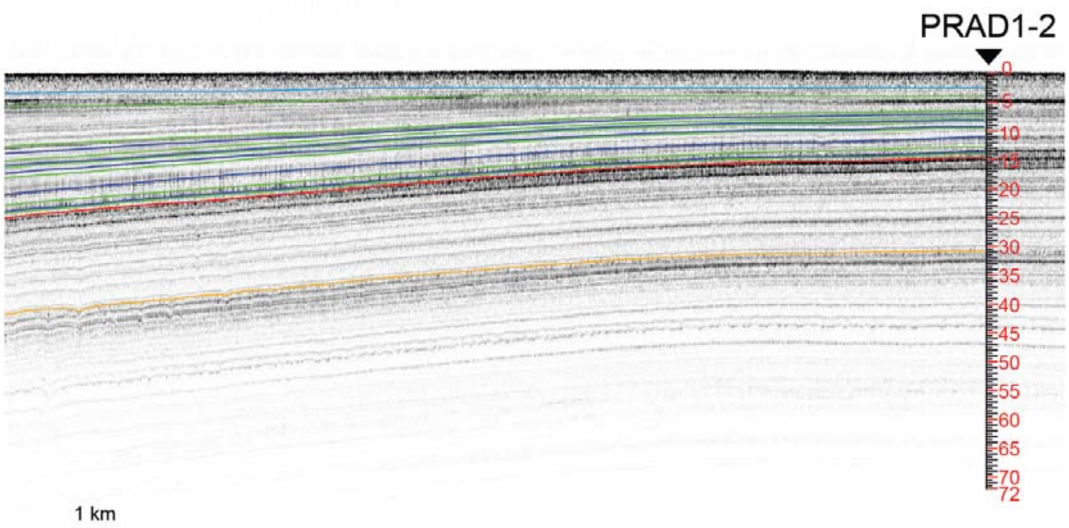

Figure DR5: Detail of CHIRP profile with same orientation of line LSD22.

CHARACTERISTIC TIMESCALE OF THE PO RIVER LOWSTAND WEDGE

We estimated the characteristic timescale threshold for each clinothems based on Sheets et al. (2002). The characteristic stratigraphic-integral timescale T_i can be expressed by the following equation: $T_i = h/\sigma$ (where h = distributary channel depth, σ = mean subsidence rate); T_i scales the transition from short-term autogenic-dominated conditions to the long-term limit in which stratigraphic patterns are controlled by allogenic factors. Considering an average h = 10 m (see Amorosi et al., 2016 for a review) and mean subsidence rate = 1.5 cm/yr (the upper limit of those observed on short time scales on the Po delta lobes; after Teatini et al., 2011) the resulting timescale threshold is 667 years; this value is reasonably close to the 450-year avulsion time scale for low-gradient deltas estimated by Reitz et al. (2015). Table DR6 and Figure DR7 display the time duration, shelf-edge progradation, and exceedance factor (relative to the calculated T_i threshold value) of each type A, B, and C clinothem for the Po River lowstand wedge.

Clinothem	Time duration (kyr)	Shelf-edge progradation (km)	Exceedance Factor
type C_2	1.4	1.1	**2.10**
type C_1	2.2	5.5	**3.30**
type A_6	0.6	3	0.90
type B_5	0.4	4	0.60
type A_5	0.3	0.5	0.45
type B_4	0.1	1.5	0.15
type A_4	1.2	1.5	**1.80**
type B_3	0.5	6.5	0.75
type A_3	3.1	3	**4.65**
type B_2	0.5	4.5	0.75
type A_2	3.7	2.4	**5.55**
type B_1	1	2.9	**1.50**
type A_1	2.4	3.9	**3.60**

Table DR6: Time interval of duration, shelf-edge progradation and exceedance factor for each clinothem. Note the exceedance factors in bold face are greater than the time scale threshold.

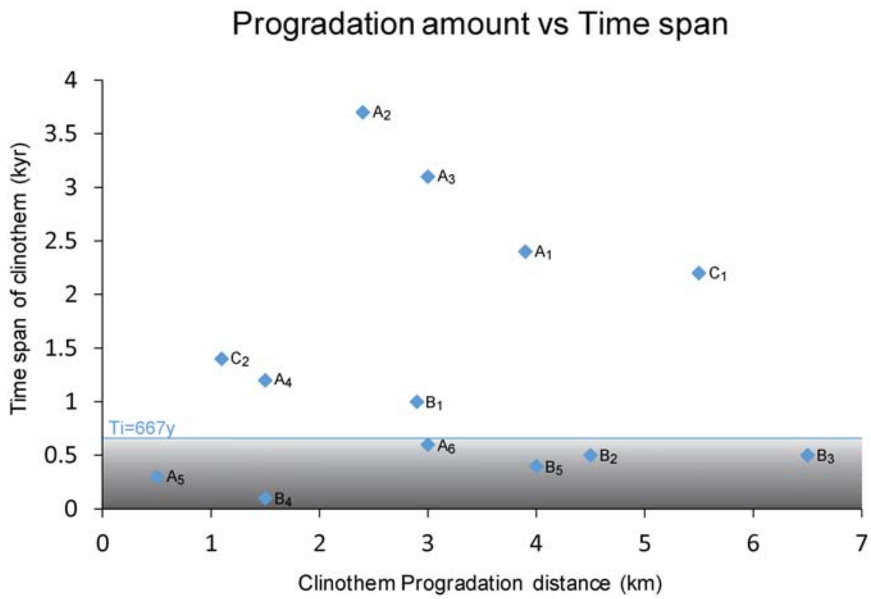

Figure DR7: Amount of progradation against time span of each clinothem relative to Ti, the stratigraphic integral timescale threshold estimated for the Po River lowstand wedge. Clinothems above the light blue line (Ti = 667 y) are more likely to preserve allogenic signals.

REFERENCES CITED

Amorosi, A., Maselli, V., Trincardi, F., 2016, Onshore to offshore anatomy of a late Quaternary source-to-sink system (Po Plain–Adriatic Sea, Italy): Earth-Science Reviews v.153, p. 212-237.

Asioli, A., Trincardi, F., Lowe, J.J., Ariztegui, D., Langone, L., and Oldfield, F., 2001, Sub-millennial scale climatic oscillations in the central Adriatic during the Late glacial: palaeoceanographic implications: Quaternary Science Reviews, v. 20(11), p. 1201-1221.

Bourne, A.J., Lowe, J.J., Trincardi, F., Asioli, A., Blockley, S.P.E., Wulf, S. Matthews, I.P. Piva, A., AND Vigliotti, L., 2010, Distal tephra record for the last ca 105,000 years from core PRAD 1-2 in the central Adriatic Sea: implications for marine tephrostratigraphy: Quaternary Science Reviews v. 29, p. 3079-3094.

Catuneanu, O., Abreu, V., Bhattacharya, J.P., Blum, M.D., Dalrymple, R.W., Eriksson, P.G., Fielding, C.R., Galloway, W.E., Gibling, M.R., Giles, K.A., Holbrook, J.M., Jordan, R., Kendall, C.G.St.C., Macurda, B., Martinsen, O.J., Miall, A.D., Neal, J.E., Nummedal, D., Pomar, L., Posamentier, H.W., Pratt, B.R., Sarg, J.F., Shanley, K.W., Steel, R.J., Strasser, A., Tucker, M.E., and Winker, C., 2009, Towards the standardization of sequence stratigraphy: Earth Science Reviews v. 92, p. 1-33.

Helland-Hansen, W., and Martinsen, O.J., 1996, Shoreline trajectories and sequences: description of variable depositional-dip scenarios: Journal of Sedimentary Research, v. 66(4), p. 670-688.

Jervey, M.T., 1988, Quantitative geological modeling of siliciclastic rock sequences and their seismic expression, in Wilgus, C.K., et al., eds., Sealevel changes: An integrated approach: Society of Economic Paleontologists and Mineralogists Special Publication v. 42, p. 47–69.

Lourens, L.J. 2004, Revised tuning of Ocean Drilling Program Site 964 and KC01B (Mediterranean) and implications for the Δ18O, tephra, calcareous nannofossil, and geomagnetic reversal chronologies of the past 1.1 Myr: Paleoceanography, v. 19, PA3010.

Maselli, V, Trincardi, F., Cattaneo, A., Ridente, D., and Asioli, A., 2010, Subsidence pattern in the central Adriatic and its influence on sediment architecture during the last 400 kyr: Journal of Geophysical Research: Solid Earth, v. 115(B12).

Matthews I.P., Trincardi F., Lowe J.J., Bourne A.J., MacLeod A., Abbott P.M., Andersen N., Asioli A., Blockley S.P.E., Lane C.S., Oh Y.A., Satow C.S., Staff R.A., and Wulf S. 2015, Developing a robust tephrochronological framework for Late Quaternary marine records in the Southern Adriatic Sea: new data from core station SA03-11: Quaternary Science Reviews, v. 118 p. 84-104.

Neal, J. and Abreu, V. 2009, Sequence stratigraphy hierarchy and the accommodation succession method. Geology, v. 37, p. 779–782.

Patruno, S., Hampson, G.J., and Jackson, C.A., 2015, Quantitative characterisation of deltaic and subaqueous clinoforms: Earth-Science Reviews, v. 142, p. 79-119.

Piva, A., Asioli, A., Schneider, R. R., Trincardi, F., Andersen, N., Colmenero-Hidalgo, E., Dennielou, B., Flores, J.A., and Vigliotti, L., 2008, Climatic cycles as expressed in sediments of the PROMESS1 borehole PRAD1-2, central Adriatic, for the last 370 ka: 1. Integrated stratigraphy: Geochemistry, Geophysics, Geosystems, v. 9(1), doi: 10.1029/2007GC001713.

Pellegrini, C., Maselli, V., Cattaneo, A., Piva, A., Ceregato, A., and Trincardi, F., 2015, Anatomy of a compound delta from the post-glacial transgressive record in the Adriatic Sea: Marine Geology, v. 362, p. 43-59.

Reimer P.J., Bard, E., Bayliss, A., Beck, J.W., Blackwell, P.G., Bronk Ramsey, C., Buck, C.E., Cheng, H., Edwards, R.L., Friedrich, M., Grootes, P.M., Guilderson, T.P., Haflidason, H., Hajdas, I., Hatte, C., Heaton, T.J., Hogg, A.G., Hughen, K.A., Kaiser, K.F., Kromer, B., Manning, S.W., Niu, M., Reimer, R.W., Richards, D.A., Scott, E.M., Southon, J.R., Turney, C.S.M., and van der

Plicht, J., 2013, IntCal13 and MARINE13 radiocarbon age calibration curves 0-50000 years calBP: Radiocarbon, v. 55, 4, p. 1869-1887.

Reitz, M.D., Pickering, J.L., Goodbred, S.L., Paola, C., Steckler, M., and Seeber, L., 2015, Effects of tectonic deformation and sea level on river path selection: theory and application to Bangladesh: Journal of Geophysical Research – Earth Surface, V. 120 (4), p. 671-689.

Ridente, D., Trincardi, F., Piva, A., and Asioli, A. 2009, The combined effect of sea level and supply during Milankovitch cyclicity: Evidence from shallow-marine δ18O records and sequence architecture (Adriatic margin): Geology, v. 37, p. 1003-1006.Sheets, B.A., Hickson, T.A., and Paola, C., 2002, Assembling the stratigraphic record: Depositional patterns and time-scales in an experimental alluvial basin; Basin Research, v. 14(3), p. 287-301.

Stuiver M. and Reimer P.J., 1993, Extended 14C data base and revised CALIB 3.0 14C age calibration program: Radiocarbon, v. 35, p. 215-230.

Teatini, P., Tosi, L., and Strozzi, T., 2011, Quantitative evidence that compaction of Holocene sediments drives the present land subsidence of the Po Delta, Italy: Journal of Geophysical Research, v. 116, B08407, doi: 10.1029/2010JB008122, 2011.

Trincardi, F., Asioli, A., Cattaneo, A., Correggiari, A., and Langone, L., 1996, Stratigraphy of the late-Quaternary deposits in the Central Adriatic basin and the record of short-term climatic events: Memorie Istituto Italaliano Idrobiologia 55, 39-70.